9-15-1989

# Hall-Effect Depletion Corrections in Ion-Implanted Samples: $Si^{29}$ in GaAs

David C. Look

*Wright State University - Main Campus*, david.look@wright.edu

# Halleffect depletion corrections in ionimplanted samples: Si29 in GaAs

D. C. Look

Citation: J. Appl. Phys. 66, 2420 (1989); doi: 10.1063/1.344250
View online: http://dx.doi.org/10.1063/1.344250
View Table of Contents: http://jap.aip.org/resource/1/JAPIAU/v66/i6
Published by the American Institute of Physics.

# Hall-effect depletion corrections in ion-implanted samples: $Si^{29}$ in GaAs

D. C. Look
*University Research Center, Wright State University, Dayton, Ohio 45435*

(Received 3 February 1989; accepted for publication 2 June 1989)

The sheet free-carrier concentration in a thin, conducting layer on an insulating substrate is lower than the net, sheet-dopant concentration because of free-carrier depletion in the surface and interface regions. Here we develop an algorithm to give the true, net sheet-donor concentration from the measured sheet-Hall concentration under the assumption of a Gaussian donor profile, which is usually sufficiently accurate for ion-implanted samples. Correction curves are generated for $Si^{29}$ ions implanted into GaAs at energies of 60, 100, 130, 150, and 200 keV, and at doses of $1\times10^{11}$–$2\times10^{14}$ ions/cm$^2$. Also, the Hall mobilities and $r$ factors are calculated at various carrier concentrations for $N_A/N_D = 0$ and $N_A/N_D = 0.5$.

## I. INTRODUCTION

Ion implantation is the technique of choice for the formation of conducting layers in a large number of present-day Si and GaAs devices. The most important figure of merit for an implantation and annealing process is the activation efficiency, i.e., the fraction of implanted ions which eventually become active dopant ions, i.e., donors or acceptors. Thus, the measurement of activation efficiency ($\eta$) is a well-studied phenomenon, and the two techniques most widely used for such studies are capacitance-voltage ($C$-$V$) measurements and Hall-effect measurements. The problems with the $C$-$V$ method are that it requires extensive sample preparation, its range of measured carrier concentrations is limited due to breakdown effects (on the high end) and series-resistance effects (on the low end), it does not give the sheet-carrier concentration directly, and it cannot be applied to all semiconductor materials. The Hall-effect method, on the other hand, suffers from none of these problems, but can be very inaccurate at low implantation doses due to the necessity of large (and unknown) surface and interface carrier-depletion corrections, and, to a lesser extent, Hall $r$-factor corrections. In this paper we address both of these problems for $Si^{29}$ implantation into GaAs, and present curves which can be used to correct experimental Hall-effect data.

## II. CALCULATION OF FREE-CARRIER DEPLETION

Consider, as a typical example, an implantation of 150-keV $Si^{29}$ ions into a semi-insulating (SI) GaAs substrate, which has a preimplantation carrier concentration $n_{sub}$ of $1\times10^{7}$ cm$^{-3}$, and a deep-donor concentration $N_{EL2}$ of $1\times10^{16}$ cm$^{-3}$. As will be shown later, these quantities, which are easily measured, are consistent with a background acceptor concentration $N_{A\text{-sub}}$ of about $1\times10^{15}$ cm$^{-3}$. Suppose also that a Hall-effect measurement gives a sheet-Hall concentration $n_{sH} = 0.97\times10^{12}$ cm$^{-2}$, and that the Hall $r$-factor can be calculated to be $r \simeq 1.03$; then the sheet-carrier concentration is $n_s = 1.00\times10^{12}$ cm$^{-2}$, and the total situation is depicted in Fig. 1, as calculated by the method described below. An assumption here is that the implanted donor profile is Gaussian and is not changed significantly by annealing; this assumption is reasonably valid for many present-day annealing processes, especially those involving the rapid-thermal-annealing (RTA) method.[1]

Because the free-surface potential $\phi_s$ (energy, $-e\phi_s$) and substrate potential $\phi_{sub}$ differ from the bulk implanted-layer potential $\phi_{ch}$, electrons will flow from the implanted layer into surface and substrate acceptor states, leaving depleted areas of widths $w_s$ and $w_i$, respectively. The electrons from the $w_i$ region fill substrate acceptor states up to a width $w_{sub}$, depending on the substrate acceptor concentration, $N_{A\text{-sub}}$. For an implantation directly into a SI GaAs substrate, the implanted-layer acceptor concentration $N_{A\text{-imp}}$ should equal $N_{A\text{-sub}}$ as long as the implantation and annealing processes do not create additional acceptors. (In Fig. 1 it is assumed that $N_{A\text{-sub}} = N_{A\text{-imp}}$.) If, on the other hand, the implantation process does create additional acceptors, then it is likely that the acceptor profile $N_A(z)$ will be much like the implanted-donor profile $N_D(z)$, especially if the acceptors involve the implant dopant ions themselves. In that

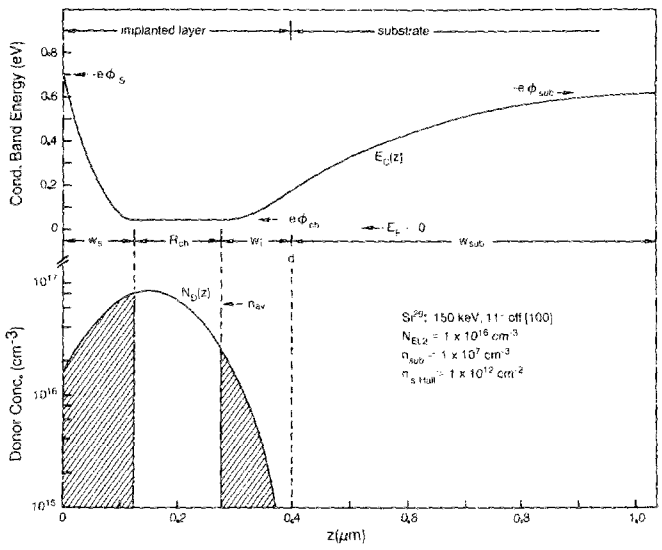


FIG. 1. The energy of the bottom of the conduction band (shown only schematically), and the donor concentration $N_D(z)$, as functions of depth for a 150-keV $Si^{29}$ implant into GaAs. It is assumed that $n_s = 1\times10^{12}$ cm$^{-2}$. The shaded regions are depleted of free electrons.

 0021-8979/89/182420-05$02.40  

case, we must take $N_D(z)$ to really mean $N_D(z) - N_A(z) \equiv N_D^{net}(z)$. The superscript "net" will not be used in the analysis following, although its potential applicability must be kept in mind. Often a mobility analysis can indicate whether or not $N_A(z)$ is appreciable.

To determine the relationships of the various potentials and depletion widths in Fig. 1 we must solve the one-dimensional Poisson's equation:

$$\frac{d^2\phi}{dz^2} = -\frac{\rho}{\epsilon} = -\frac{e}{\epsilon}(N_D^+ - N_A^- + p - n), \tag{1}$$

where $\phi$ is the electrostatic potential and $\epsilon = 1.143\times10^{-10}$ F/m in GaAs. By multiplying both sides by $z$ and integrating from $a$ to $b$, we get

$$b\phi'(b) - a\phi'(a) - \phi(b) + \phi(a) = -\frac{e}{\epsilon}\int_a^b z(N_D^+ - N_A^- + p - n)dz, \tag{2}$$

where $\phi'(z) \equiv d\phi/dz$. A tractable solution of Eq. (2) is possible if we can apply the depletion approximation, i.e., if $\phi'(w_s) = \phi'(d - w_i) = \phi'(d + w_{sub}) = 0$, and if $p - n \simeq 0$ everywhere except for the region $w_s < z < d - w_i$. The depletion approximation should be reasonably valid as long as the channel width $R_{ch}$ is at least several Debye lengths ($\lambda_D$'s). For the conditions used in Fig. 1, $R_{ch} \simeq 1535$ Å and $\lambda_D \simeq 167$ Å (at $n_{av}$), so that the depletion approximation should not introduce a significant error. For higher carrier concentrations, which are more usual in ion-implanted samples, the approximation is even better. Thus, we have

$$-\phi_{ch} + \phi_s = -\frac{kT}{e} - \frac{e}{\epsilon}\int_0^{w_s} z[N_D(z) - N_{A\text{-imp}}]dz, \tag{3}$$

$$-\phi_{sub} + \phi_{ch} = \frac{kT}{e} - \frac{e}{\epsilon}\left(\int_{d-w_i}^{d} z[N_D(z) - N_{A\text{-imp}}] - \int_d^{d+w_{sub}} zN_{A\text{-sub}}\,dz\right), \tag{4}$$

where the $kT/e$ term can be taken as a partial correction for the assumption of "abrupt" depletion walls, since the free electrons will actually "leak" a few Debye lengths into the depletion regions. A third equation invokes the change-conservation requirement:

$$\int_{d-w_i}^{d}[N_D(z) - N_{A\text{-imp}}]dz = \int_d^{d+w_{sub}} N_{A\text{-sub}}\,dz, \tag{5}$$

and, finally, we can introduce a relationship for the measured sheet-carrier concentration $n_s$:

$$n_s = \int_{w_s}^{d-w_i}[N_D(z) - N_{A\text{-imp}}]dz. \tag{6}$$

By simple algebra and changes of variables in the integrals it can be shown that

$$-\phi_s + \phi_{ch} - \frac{kT}{e} = \frac{e}{\epsilon}\left(I_2 - \frac{w_s^2}{2}N_{A\text{-imp}}\right), \tag{7}$$

$$-\phi_{sub} + \phi_{ch} - \frac{kT}{e} = \frac{e}{\epsilon}\left[-I_4 + \frac{I_3^2}{2N_{A\text{-sub}}} - \left(w_iI_3 - \frac{w_i^2}{2}N_{A\text{-imp}}\right)\times\left(\frac{N_{A\text{-imp}}}{N_{A\text{-sub}}} - 1\right)\right], \tag{8}$$

$$n_s = I_0 - I_1 - I_3 - (d - w_s - w_i)N_{A\text{-imp}}, \tag{9}$$

where

$$I_0 = \int_0^d N_D(z)dz, \tag{10}$$

$$I_1 = \int_0^{w_s} N_D(z)dz, \tag{11}$$

$$I_2 = \int_0^{w_s} zN_D(z)dz, \tag{12}$$

$$I_3 = \int_0^{w_i} N_D(z + d - w_i)dz, \tag{13}$$

$$I_4 = \int_0^{w_i} zN_D(z + d - w_i)dz. \tag{14}$$

Note that if $N_D$ is *uniform* in a layer of thickness $d$, then Eqs. (7) and (8) become

$$-\phi_s + \phi_{ch} - \frac{kT}{e} = \frac{e}{\epsilon}\frac{w_s^2}{2}(N_D - N_{A\text{-layer}}), \tag{15}$$

$$-\phi_{sub} + \phi_{ch} - \frac{kT}{e} = \frac{e}{\epsilon}\frac{w_i^2}{2}\left[(N_D - N_{A\text{-layer}})\times\left(1 + \frac{N_D - N_{A\text{-layer}}}{N_{A\text{-sub}}}\right)\right]. \tag{16}$$

These are the familiar equations often used for depletion corrections,[2] although Eq. (16) is usually evaluated in the limit $N_{A\text{-sub}} \gg N_D - N_{A\text{-layer}}$, for two reasons: (1) $N_{A\text{-sub}}$ is not known or (2) it is assumed that *interface* states, rather than substrate acceptors, accomodate most of the depletion electrons. Without further knowledge, it is difficult to avoid this uncertainty in the consideration of interface depletion.

For the implanted layers, we will assume a Gaussian form for the donor concentration:

$$N_D(z) = C\exp\left[-\frac{1}{2}\left(\frac{z - R_p}{\Delta R_p}\right)^2\right], \tag{17}$$

where $R_p$ is the range and $\Delta R_p$ the standard deviation of the distribution. Accurate Gaussian representations of actual ion-implantation profiles are available in the literature.[3] However, any other profile can also be used to form the integrals $I_0$-$I_4$, Eqs. (10)–(14), respectively. For the Gaussian profile the total sheet donor concentration is

$$N_D(z) = \int_0^{R_p + 3\Delta R_p} C\exp\left[-\frac{1}{2}\left(\frac{z - R_p}{\Delta R_p}\right)^2\right]dz = CI_0, \tag{18}$$

where, to facilitate a computer calculation, we are normalizing the distribution in a depth $d = R_p + 3\Delta R_p$. The constant $C$ is quite close to the value $N_{Ds}/\sqrt{(2\pi)}\Delta R_p$.

The potentials are given as follows: First, we estimate[4] that the free-surface potential $\phi_s$ is about $-0.7$ V. Next, we write the channel potential $\phi_{ch}$ as

$$\phi_{ch} = -\frac{kT}{e}\left[\ln\left(\frac{N_C}{n_{av}}\right) - \frac{n_{av}}{\sqrt{8}N_C}\right], \tag{19}$$

where $n_{av} = n_s/(d - w_s - w_i) = n_s/R_{ch}$, and $N_C$ is given[5] by

$$N_C = 8.63\times10^{13}\, T^{3/2}\,(1-1.93\times10^{-4}\, T - 4.19\times10^{-8}\, T^2). \quad (20)$$

This expression[6] for $\phi_{ch}$ is sufficiently accurate for $n < 4\times10^{18}$ cm$^{-3}$ at 296 K, and for $n < 6\times10^{17}$ cm$^{-3}$ at 77 K. However, at 296 K the Fermi energy crosses the conduction-band edge at $n \simeq 3.1\times10^{17}$ cm$^{-3}$, and at 77 K, $4.4\times10^{16}$ cm$^{-3}$. At higher concentrations than these we set $\phi_{ch} = 0$ in Eqs. (7) and (8), since the relevant barriers should then be measured from the Fermi level, not the bottom of the conduction band; thus, Eq. (19) is a sufficient approximation for these purposes.

Finally, the substrate potential $\phi_{sub}$ may be determined from the relationship $\phi_{sub} = -E_F/e$, where the Fermi energy $E_F$ is given[7] by

$$n_{sub} = N_C e^{-E_F/kT} = \frac{g_0}{g_1}\left(\frac{N_{EL2}}{N_{A\text{-sub}}} - 1\right) N_C e^{-E_{EL2}/kT}. \quad (21)$$

Here, $g_0/g_1 = 1/2$ for the deep donor EL2 in undoped, SI GaAs, and the EL2 energy can be roughly determined from

$$E_{EL2} \simeq \{0.65 + 0.10[(296 - T)/296)]\}\text{eV}. \quad (22)$$

Equation (22) assumes a linear interpolation between the known 0-K value[8] $E_{EL2}(0) \simeq 0.75$ eV, and the estimated 296-K value[9] $E_{EL2}(296) \simeq 0.65$ eV. Since it is relatively easy to measure $n_{sub}$ at 296 K, but nearly impossible to measure $n_{sub}$ below 200 K, we estimate $n_{sub}$ at lower temperatures by

$$n_{sub}(T) = [2.764\times10^{-7} N_C(T) e^{-E_{EL2}(T)/kT}]\, n_{sub}(296), \quad (23)$$

where all concentrations are measured in cm$^{-3}$. Then $\phi_{sub}$ becomes

$$\phi_{sub} = -\frac{E_F}{e} = -\frac{kT}{e}\ln\left(\frac{N_C(T)}{n_{sub}(T)}\right). \quad (24)$$

Since $N_{EL2}$ does not vary widely in SI GaAs (about $1.0 \pm 0.3\times10^{16}$ cm$^{-3}$), and in any case is easily measured either by 1.1-$\mu$m absorption or DLTS, it is convenient to determine $N_{A\text{-sub}}$ from $n_{sub}$ and $N_{EL2}$ by using Eq. (21):

$$N_{A\text{-sub}} \simeq \frac{N_{EL2}}{1 + 5.53\times10^{-7} n_{sub}(296)}, \quad (25)$$

where $n_{sub}(296)$ is measured in cm$^{-3}$. The reason for using $n_{sub}(296)$ to determine $\phi_{sub}$ and $N_{A\text{-sub}}$ is that most implantation groups will usually measure $n_{sub}(296)$ on a separate piece of the same wafer, or at least on a piece of a nearby wafer, before commencing the implantation process. It should also be noted that if $N_{EL2}$ is measured by 1.1-$\mu$m absorption, the quantity actually measured is $N^0_{EL2}$, the neutral fraction of $N_{EL2}$. Since $N^0_{EL2} = N_{EL2} - N_{A\text{-sub}}$, it is easy to write Eqs. (21) and (25) in terms of $N^0_{EL2}$, by dropping the "1" in each case.

The quantity of interest in practical implantation studies is the activation efficiency $\eta \equiv N_{Ds}/N_{dose}$, where $N_{dose}$ is the number of ions implanted per unit area. To determine $N_{Ds}$ we must find $C$ in Eq. (18). (Note that the quantities $R_p$ and $\Delta R_p$ are available in tables or can be calculated[3]; they depend on ion mass, host composition, implant energy, and implant angle.) To determine $C$, it is necessary to vary $C$, $w_s$, and $w_i$ until Eqs. (7), (8), and (9) are all satisfied simultaneously. We have written a computer program in Interpreted GW BASIC which typically finds $N_{Ds}$ to better than 1% accuracy in about 20 s on a PC/AT-type computer. Multiple solutions are sometimes possible, especially if $N_{A\text{-imp}} \neq N_{A\text{-sub}}$, although usually it is easy to tell which solution is correct. For a direct-implant process, $N_{A\text{-imp}} = N_{A\text{-sub}}$ of course, since the background acceptor concentrations should be the same.

## III. COMPLICATIONS OF THE HALL-EFFECT EXPERIMENT

The determination of the sheet-carrier concentration $n_s$ by the Hall effect is complicated by two factors: (1) the quantity which is actually measured is not $n_s$ but is $n_{sH} = n_s/r$, where $r$ is the so-called "Hall $r$ factor"; and (2) the carrier concentration $n$ is not uniform in the channel region. We have calculated $r$ by a numerical solution of the Boltzmann transport equation[10] for various values of *volume* carrier concentration $n$ and compensation ratio $N_A/N_D$ in $n$-type GaAs. The results, shown in Fig. 2, can be used in the following ways: (1) First, it is assumed that $r = 1$, i.e., $n_s = n_{sH}$, and Eqs. (7)–(9) are solved to give $w_s$ and $w_i$; (2)

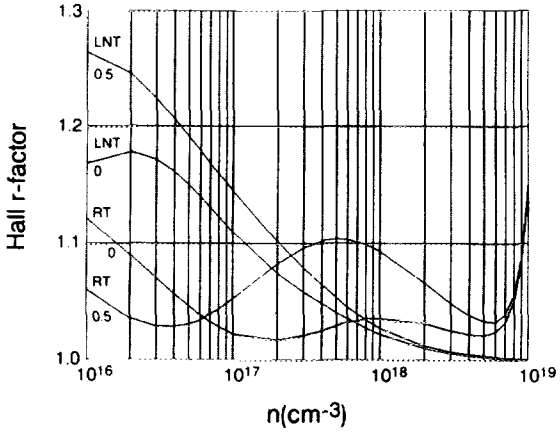


FIG. 2. The Hall $r$-factor, for temperatures of 296 and 77 K, and compensation ratios of 0 and 0.5, as a function of *volume* carrier concentration $n$.

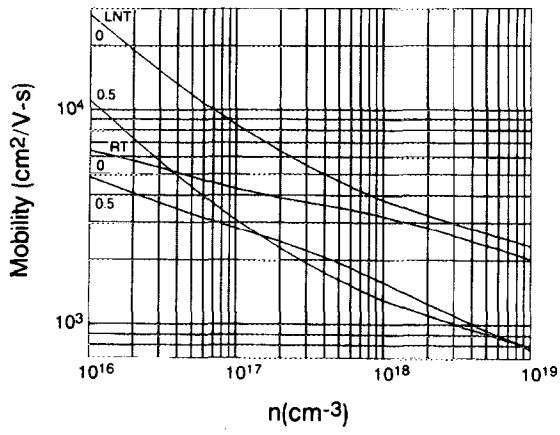


FIG. 3. The Hall mobility, for temperatures of 296 and 77 K, and compensation ratios of 0 and 0.5, as a function of *volume* carrier concentration $n$.

then, $n_{av}$ is calculated from $n_{av} = n_s/(d - w_s - w_i)$; (3) finally, $r$ is estimated from Fig. 2, and a new value of $n_s$ is then calculated; i.e., $n_s = rn_{sH}$. Usually, another iteration of $n_s$ and $r$ is not necessary.

The second problem, the carrier nonuniformity, results in the sheet Hall concentration $n_{sH}$ (or the Hall coefficient $R_H$) being a weighted average of the true volume carrier concentration $n(z)$:

$$n_{sH} \equiv \frac{1}{eR_H} = \frac{1}{e}\frac{\left[\int_{w_s}^{d-w_i}\sigma(z)dz\right]^2}{\int_{w_s}^{d-w_i}R_H(z)\sigma^2(z)dz} = \frac{\left[\int_{w_s}^{d-w_i}n(z)\mu(z)dz\right]^2}{\int_{w_s}^{d-w_i}r(z)n(z)\mu^2(z)dz} < \frac{1}{r(n_{av})}\int_{w_s}^{d-w_i}n(z)dz = \frac{n_s}{r(n_{av})}, \quad (26)$$

where, in the fifth term, we have assumed that $r(z)$ is approximately constant in the channel region, and where the inequality results from a well-known theorem of integrals. Fortunately, however, the mobility weighting is usually not important, at least for 296-K results. As an example, we can apply the calculated $r$-factor and mobility curves of Figs. 2 and 3 to the carrier concentration data of Fig. 1 ($n = N_D - N_A$) to show that the weighted sheet carrier concentration [fourth term in Eq. (26)] is only 0.5% smaller than the unweighted concentration (fifth term). [As a more extreme example, suppose that a hypothetical layer has a uniform carrier concentration, but that half of the layer has a mobility twice as high as that of the other half. Even in this case, the weighted concentration, from Eq. (26), is only 10% smaller than the unweighted concentration.] The above examples thus indicate that this problem is usually not important; however, for maximum accuracy one could carry out a numerical integration of Eq. (26) with the curves of Figs. 2 and 3.

## IV. RESULTS AND DISCUSSION

The equations of this paper are solved at 296 K for $Si^{29}$, implanted into GaAs at 11° off a [100] direction, and at energies of 60, 100, 130, 150, and 200 keV, as displayed from top to bottom in Fig. 4. (Note the scale changes.) It is assumed here that $N_{EL2} = 1.0\times10^{16}\,cm^{-3}$ and $n_{sub} = 1\times10^{7}$ $cm^{-3}$, typical values in present day SI GaAs. Thus, for example, if a $2\times10^{12}\,cm^{-2}$ implant, at 150 keV, produced a measured sheet-carrier concentration of $1\times10^{12}\,cm^{-2}$, the correct $N_{Ds}$ would be about $1.96\times10^{12}\,cm^{-2}$, and thus the efficiency, about 98%. These curves will change, of course, for different values of $N_{sub}$ and $N_{EL2}$, so they should be viewed only as a guide to the magnitude of the depletion corrections. Also, the curves should not be considered accurate for $n_s \leqslant 2\times10^{11}\,cm^{-2}$, since then $R_{ch}/\lambda_D \leqslant 3$ and the depletion approximation fails.

As a final example, we present data from an undoped, SI GaAs wafer which was implanted with $2\times10^{12}\,cm^{-2}$, $Si^{29}$ ions at 150 keV, 11° off the [100] direction, and annealed at 900 °C for 10 s by a rapid thermal process. Further results from this and other samples, annealed at different temperatures, will be published elsewhere. The data are summarized in Table I. Note that the $r$-factor correction is only about 3%, while the depletion correction is much larger. The final efficiency, 86%, denotes a good implantation process, whereas the uncorrected value, 47%, would have given the wrong impression, i.e., that the process had severe problems. Note that, in theory, the 86% measured activation could actually represent 100% activation of $N_D$, if there were a corresponding 14% reduction due to the production of implantation-defect acceptors, which had the same Gaussian profile as $N_D(z)$. However, this scenario is unlikely in this case, because the Hall mobility turns out to be a high value, $4.01\times10^{3}\,cm^2/V\,s$, which according to Fig. 3 suggests very low compensation.

## V. CONCLUSIONS

We have developed a model which corrects the sheet Hall concentration for depletion effects in the case of a Gaussian donor distribution. (The model could easily be generalized for other distributions, since it involves numerical integrations anyway.) Other corrections, such as the Hall $r$ factor, and the effects of nonuniform carrier distribution on the Hall coefficient, have also been considered. The model is

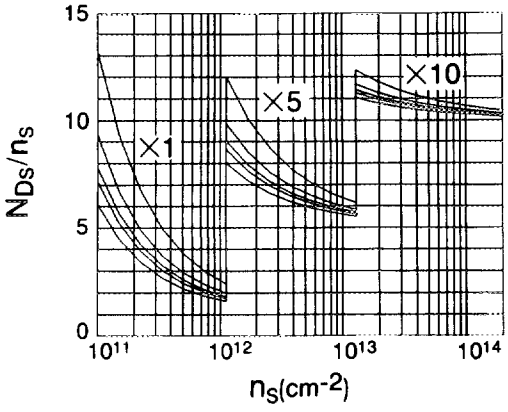


FIG. 4. The depletion correction factors as a function of *sheet* carrier concentration $n_s$ for implant energies of 60, 100, 130, 150, and 200 keV, from top to bottom. Note the scale changes. The curves should not be considered accurate for $n_s < 2\times10^{11}\,cm^{-2}$, since then $R_{ch}/\lambda_D < 3$ and the depletion approximation fails.

TABLE I. Data from an undoped, SI GaAs wafer implanted with $2\times10^{12}$ $cm^{-2}$ $Si^{29}$ ions at 150 keV, 11° off the [100] direction. Measured values of $n_{sub}$ and $N_{EL2}$ were $1.7\times10^{7}$ and $1.0\times10^{16}\,cm^{-3}$, respectively.

| | $n_s(10^{12}\,cm^{-2})$ | | | |
|---|---|---|---|---|
| $T$ (K) | Raw Hall data | With $r$-factor correction | $N_{Ds}$ ($10^{12}\,cm^{-2}$) | $\eta \equiv N_{Ds}/\text{dose}$ |
| 296 | 0.946 | 0.980[a] | 1.73[b] | 86% |

[a] From raw Hall data and Fig. 2, assuming $n_{av} \simeq n_{s\text{-raw}}/(d - w_s - w_i) \simeq 6.2\times10^{16}\,cm^{-3}$, and $N_A/N_D \simeq 0$.

[b] From $r$-factor-corrected Hall data and fit of Eqs. (7)–(9). (Also, Fig. 4 gives a good approximation, even though $n_{sub}$ is different.)

applied to ion-implanted GaAs samples, and charts are given to predict the corrections under typical conditions.


## ACKNOWLEDGMENTS

The author would like to thank J. Crist for helpful discussions, J. S. Sizelove for the mobility and $r$-factor plots, J. Farmer for ion implantation, and T. Cooper for Hall-effect measurements. The work was performed at the Electronic Technology Laboratory, Wright-Patterson AFB, under US Air Force Contract No. F33615-86-C-1062.



[1]S. J. Pearton, K. D. Cummings, and G. P. Vella-Coleiro, J. Appl. Phys. **58**, 3252 (1985).

[2]A. Chandra, C. E. C. Wood, D. W. Woodard, and L. F. Eastman, Solid-State Electron. **22**, 645 (1979).

[3]We have used a computer program "Ion Implant Profile code, V.2," from Implant Sciences Corp., Danvers, MA.

[4]W. E. Spicer, I. Lindau, P. Skeath, and C. Y. Su, J. Vac. Sci. Technol. **17**, 1019 (1980).

[5]J. S. Blakemore, J. Appl. Phys. **53**, R123 (1982).

[6]H. Kroemer, J. Appl. Phys. **52**, 873 (1981).

[7]D. C. Look, *Electrical Characterization of GaAs Materials and Devices* (Wiley, New York, 1989), p. 117.

[8]D. C. Look, in *Semiconductors and Semimetals*, Vol. 19, edited by R. K. Willardson and A. C. Beer (Academic, New York, 1983), p. 93.

[9]W. M. Duncan and G. H. Westphal, in *GaAs and Related Compounds, 1986*, edited by W. T. Lindley, Inst. of Phys. Conf. Ser. No. 83 (IOP, Bristol, 1987), p. 39.

[10]D. C. Look, *Electrical Characterization of GaAs Materials and Devices* (Wiley, New York, 1989), p. 93.